10:18:11 OCA PAD INITIATION - PROJECT HEADER INFORMATION 06/19/90

Active

Project #: E-21-F72 Cost share #: Rev #: 0
Center # : 10/24-6-R6972-1A0 Center shr #: OCA file #:
Work type : RES
Contract#: 1 S15 HL45767-01 Mod #: Document : GRANT
Prime #: Contract entity: GTRC

Subprojects ? : N
Main project #:

Project unit: EE Unit code: 02.010.118
Project director(s):
HUNT W D EE (404)894-2945

Sponsor/division names: DHHS/PHS/NIH / NATL INSTITUTES OF HEALTH
Sponsor/division codes: 108 / 001

Award period: 900801 to 910731 (performance) 911031 (reports)

Sponsor amount	New this change	Total to date
Contract value	21,539.00	21,539.00
Funded	21,539.00	21,539.00
Cost sharing amount		0.00

Does subcontracting plan apply ?: N

Title: PROGRAMMABLE FUNCTION GENERATOR & DIGITAL OSCILLOSCOPE

PROJECT ADMINISTRATION DATA

OCA contact: Kathleen R. Ehlinger 894-4820

Sponsor technical contact

DR. HENRY G. ROSCOE
(301)496-7225

NATIONAL INSTITUTES OF HEALTH
NATIONAL HEART, LUNG, AND BLOOD
INSTITUTE
DIVISION OF EXTRAMURAL AFFAIRS
BETHESDA, MD 20892

Sponsor issuing office

MARGARET E. HEYDRICK
(301)496-7255

NATIONAL INSTITUTES OF HEALTH
GRANTS OPERATION BRANCH
NATIONAL HEART, LUNG, & BLOOD INSTIT
5333 WESTBARD AVENUE
BETHESDA, MD 20892

Security class (U,C,S,TS) : U ONR resident rep. is ACO (Y/N): N
Defense priority rating : N/A NIH supplemental sheet
Equipment title vests with: Sponsor GIT X

Administrative comments -
INITIATION OF PROJECT. USE OF FUNDS IS RESTRICTED TO PURCHASE OF EQUIPMENT IDENTIFIED IN THE GRANT APPLICATION. SEE NOTICE OF AWARD FOR DETAILS.

GEORGIA INSTITUTE OF TECHNOLOGY
OFFICE OF CONTRACT ADMINISTRATION

NOTICE OF PROJECT CLOSEOUT

Closeout Notice Date 01/20/93

Project No. E-21-F72 Center No. 10/24-6-R6972-1A0

Project Director HUNT W D School/Lab ELEC ENGR

Sponsor DHHS/PHS/NIH/NATL INSTITUTES OF HEALTH

Contract/Grant No. 1 S15 HL45767-01 Contract Entity GTRC

Prime Contract No.

Title PROGRAMMABLE FUNCTION GENERATOR & DIGITAL OSCILLOSCOPE

Effective Completion Date 910731 (Performance) 911031 (Reports)

Closeout Actions Required:	Y/N	Date Submitted
Final Invoice or Copy of Final Invoice	Y	
Final Report of Inventions and/or Subcontracts	Y	
Government Property Inventory & Related Certificate	N	
Classified Material Certificate	N	
Release and Assignment	N	
Other	N	

CommentsUSE FORM HHS568 FOR PATENT REPORT. CONTRACT VALUE $21,539.
EFFECTIVE DATE 8-1-90.

Subproject Under Main Project No.

Continues Project No.

Distribution Required:

Project Director	Y
Administrative Network Representative	Y
GTRI Accounting/Grants and Contracts	Y
Procurement/Supply Services	Y
Research Property Managment	Y
Research Security Services	N
Reports Coordinator (OCA)	Y
GTRC	Y
Project File	Y
Other HARRY VANN-FMD	Y
FRED CAIN-OOD	Y

NOTE: Final Patent Questionnaire sent to PDPI.

Georgia Tech

School of Electrical Engineering

Georgia Institute of Technology
Atlanta, Georgia 30332-0250
Fax 404•853•9171

December 3, 1992

Dr. Henry G. Roscoe
National Institute of Health
National Heart, Lung, and Blood Institute
Division of Extramural Affairs
Bethesda, Maryland 20892

SUBJECT: Final Technical Report for Contract # 1 S15 HL45767-01, administered by Dr. William D. Hunt

Attached as required by Contract, are three copies of subject report above.

Should you have questions or need additional information, please call me at (404) 853-9452.

Kathy Knighton
Administrative Assistant

FINAL REPORT

NIH Program: Small Instrumentation Grant Program
Division of Heart and Vascular Diseases
National Heart, Lung and Blood Institute

Project Title: Programmable Function Generator and Digital Oscilloscope

NIH Project #: 1 S15 HL45767-01

Principal Investigator: William D. Hunt
Associate Professor
School of Electrical Engineering
Atlanta, Georgia 30332-0250

Funding: $21,539

Grant Period: August 1, 1990 to July 31, 1991

RESEARCH DESCRIPTION:

The research efforts supported by this equipment grant are in the area of biomedical ultrasound. These projects involve among others:

- the development of new transducer designs for transcutaneous and intravascular ultrasound

- the development of ultrasound systems for disease-specific tissue characterization

- transducer designs for ultrasonic hypothermia

One project which has made substantial use of the equipment is a project to develop a catheter tip acoustic microscope for use in the prediction of pulmonary artery growth potential in children with congenital cardiovascular defects including truncus arteriosus, tetralogy of Fallot and interrupted aortic arch. This project has been funded by the Georgia Tech/Medical College of Georgia Biomedical Research and Education Program. The co-investigators for this project are Professor William Hunt of Georgia Tech and Dr. David Connuck of the Pediatric Cardiology group at the Medical College of Georgia.

Some of the papers which have been generated as a result of this NIH equipment grant are included in Appendix A.

EQUIPMENT:

Bids were taken and a careful evaluation of the vendor responses was made including a number of on-site demonstrations. Based on our evaluation the equipment selected under this project included a Tektronix 2432A digitizing oscilloscope and a Analogic 2020 Polynomial Waveform Synthesizer (programmable function generator). With this system we are able to measure the acoustic beam profiles associated with various transducer designs. The programmable function generator allows us to investigate various signal schemes for tissue characterization such as FM chirps. The digitizing oscilloscope allows us to process ultrasonic echoes from tissue and determine the most advantageous signal processing schemes.

APPENDIX A: RELATED PAPERS

DESIGN AND CONSTRUCTION OF A PVDF FRESNEL LENS

M. Z. Sleva and W. D. Hunt

School of Electrical Engineering and Microelectronics Research Center
Georgia Institute of Technology, Atlanta, Georgia 30332-0250, USA

Abstract

The design, construction, and performance of an experimental broadband polyvinylidene flouride (PVDF) Fresnel lens are discussed. Since PVDF is characterised by an acoustic impedance which is closely matched with that of human tissue, this work is motivated by the potential application of a lens of this type in medical imaging, particularly for shallow features such as the carotid artery. A model for the lens is proposed. A general pressure transfer function is derived, which is used to obtain theoretical on-axis and focal plane beam profiles. Two identical lenses were tested in a water tank, and experimental self-convolution profiles are reported.

I. Introduction

The objective of this work is to build an experimental wideband Fresnel lens using polyvinylidene flouride (PVDF) and to investigate the theoretical and experimental beam profiles of the lens. The long-term goal is to use a lens of this type for imaging shallow features such as the carotid artery. PVDF was chosen, primarily, because of its acoustic impedance (~ 4 MRayls), which is closely matched with that of human tissue and water (~ 1.5 MRayls). In addition, it has been reported extensively that PVDF transducers exhibit wideband performance when properly designed [1].

A disk-shaped transducer may be used to realise an acoustic Fresnel lens by depositing or etching a Fresnel zone plate (FZP) electrode pattern on one face of the transducer while maintaining a full electrode on the opposite face as illustrated in Fig. 1. The radii which define the pattern and, consequently, the ring-shaped zone boundaries are determined from Fresnel diffraction theory [2], and are given by:

$$r_m = \left[\frac{m\lambda}{2}\left(z_o + \frac{m\lambda}{8}\right)\right]^{1/2} \quad ; \quad m = 1, 3, 5, \ldots \qquad (1)$$

where z_o is the focal length, and λ is the acoustic wavelength in the medium into which the transducer is radiating. The zone plate electrode pattern is an amplitude grating since acoustic signals are excited only from those zones which are covered by the electrode. Ideally, the excited signals are of equal amplitude and are in phase.

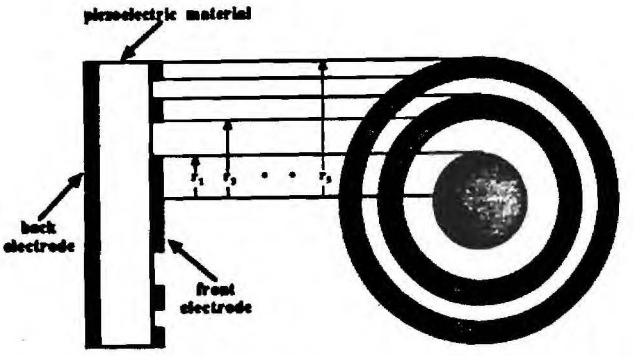

Figure 1: Zone plate configuration and definition of zone boundaries.

An alternative method of synthesising an acoustic lens is to use a Fresnel phase plate (FPP), which is a phase grating also described by Eq. (1). For a phase plate, all of the zones excite acoustic signals of equal amplitude; however, a π phase shift is introduced between the signals generated at adjacent zones. The phase shift may be obtained electrically by either driving adjacent zones in anti-phase or by poling adjacent zones anti-parallel to one another [3]. Alternatively,

1051-0117/90/0000-0821 $1.00 © 1990 IEEE

the phase shift may be obtained acoustically by etching grooves in a seperate material to provide a π phase retardation between adjacent sones. The grooved material is then affixed to the transducer [4,5]. At frequencies useful for imaging, it would be difficult to provide adequate electrical isolation between adjacent sones using the former methods since the dimensions of the pattern would be relatively small. Using the latter method with a PVDF transducer, the required groove depth is too great to etch chemically for any useful lens material (e.g., lucite). In addition it would be difficult to adequately pack the grooves with coupling gel in a clinical situation. For these reasons it was decided to use a sone plate, which is relatively easy to fabricate. The remainder of this paper discusses the modelling, construction, and performance of a PVDF sone plate.

II. Development Of Transfer Function

For a practical application, a lens is designed to meet predetermined physical specifications and focusing performance characteristics, which typically include operating frequency, F-number, focal length, side-lobe levels, and depth of focus. The beamwidth and side-lobe levels ultimately determine the achievable resolution in the transverse direction. The depth of focus determines the achievable axial resolution provided the transducer has sufficient bandwidth. It is of interest then to determine, during the design phase, if the required focusing performance can be achieved for a given F-number at the frequency of interest. Quantitative asessments of the focal point location and depth of focus may be obtained from the relative pressure distribution or beam profile on the lens axis. Likewise, quantitative assessments of beamwidth and side-lobe levels can be made from the focal plane beam profile. Both beam profiles may be generated from a general pressure transfer function.

To calculate a transfer function relating the pressure at an arbitrary point to the pressure at the lens, the lens is modelled as a series of concentric, ring-shaped radiators mounted on an infinite, rigid baffle. All radiators are assumed to be uniformly excited with equal amplitude and in phase. In addition, it is assumed that the spatial distribution of the acoustic field immediately in front of the lens is an exact replica of the FZP electrode pattern. It has been shown that the latter assumption, which neglects mechanical aberrations, may result in inaccurately computed beam profiles [6]. The aberrations are caused by the finite spatial cut-off frequency of the transducer material and reflections at the front and rear of the transducer due to impedance mismatches [7]. The design used in this work takes advantage of the low acoustic impedance of PVDF to circumvent the problem of multiple reflections. The lens is backed with an impedance matched material, resulting in negligible reflections at the rear. The impedance ratio of PVDF to water is about 2.7:1, resulting in a normal reflection coefficient of magnitude 0.45 at the front interface, so reflections at the front face of the lens are minimal. The cut-off frequency, however, is a function of material properties of the PVDF [3,6].

For the general case of a radiator of area S_o mounted on an infinite, rigid baffle in the z=0 plane and uniformly excited with an impulsive velocity, $\vec{v} = v_o\delta(t)\hat{z}$, the potential at an arbitrary point B at $\vec{r}$, is given by the Rayleigh Integral:

$$\varphi(t,\vec{r}) = \frac{v_o}{2\pi}\iint_{S_o}\frac{\delta\left(t-\frac{R}{V_\ell}\right)}{R}dS. \tag{2}$$

In Eq. (2) V_ℓ is the speed of sound in the medium (in this work, taken to be water). The integration need be carried out only over S_o, as this is the only surface for which the integrand is nonsero since it is assumed that the Sommerfeld radiation condition applies and that the baffle is rigid. From Eq. (2) the required transfer function is found to be:

$$\frac{P(\omega,\vec{r})}{P_o} = \frac{j\omega}{2\pi V_\ell}\iint_{s_o}\frac{e^{-j\omega R/V_\ell}}{R}dS \tag{3}$$

where P and P_o are the pressures at point B and at the face of the transducer, respectively.

Equation (3) can be applied directly to the case of an FZP if S_o is the area defined by the sone plate electrode pattern. This is carried out by calculating the individual contributions to the total pressure at a given point from each radiating ring (sone) and then summing all the contributions. The geometry appropriate for calculation of the pressure at an arbitrary point due to a single ring-shaped radiator is shown in Fig. 2. Using cylindrical coordinates as defined in the figure, $P(\omega,\vec{r}) = P(\omega,r_c,\phi,z)$. The on-axis response for the n^{th} ring-shaped radiator is found in closed form as:

$$\frac{P_n(\omega,0,0,z)}{P_o} = j\sin\frac{\omega u_{b_n}}{V_\ell} - j\sin\frac{\omega u_{a_n}}{V_\ell} - \cos\frac{\omega u_{b_n}}{V_\ell} + \cos\frac{\omega u_{a_n}}{V_\ell} \tag{4}$$

where $u_{a_n} = \left(a_n^2 + z^2\right)^{1/2}$ and $u_{b_n} = \left(b_n^2 + z^2\right)^{1/2}$. The total pressure at a point on the z-axis due to a plate with N sones then is given by the following summation:

$$\frac{P(\omega,0,0,z)}{P_o} = \sum_{n=1}^{N}\left[j\sin\frac{\omega u_{b_n}}{V_\ell} - j\sin\frac{\omega u_{a_n}}{V_\ell} - \cos\frac{\omega u_{b_n}}{V_\ell} + \cos\frac{\omega u_{a_n}}{V_\ell}\right]. \quad (5)$$

Setting $z = z_o$ in the expressions for u_{a_n} and u_{b_n} obtains the total pressure at the focal point. For a point off-axis, Eq. (3) must be evaluated numerically. For a zone plate with N zones, the total pressure at a point in the focal plane is given by:

$$\frac{P(\omega,r_c,\phi,z_o)}{P_o} = \sum_{n=1}^{N}\left[\int_0^{2\pi}\int_{a_n}^{b_n}\frac{e^{-j\omega R/V_\ell}}{R}r_c' dr_c' d\phi'\right] \quad (6)$$

where the primed variables refer to the radiator surface.

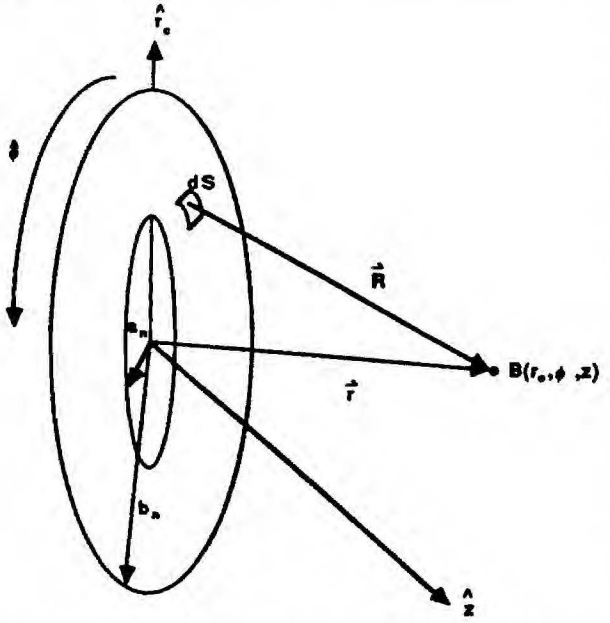

Figure 2: Geometry for calculation of pressure at arbitrary point B due to a single ring-shaped radiator.

III. Calculated Beam Profiles

A 7 zone, 15 mm diameter zone plate was designed for a focal length of 27.2 mm (F-number =1.81) at a center frequency of 10 MHz, which is the half-wavelength resonance frequency for a 110 μm thick sample of PVDF. The on-axis beam profile is shown in Fig. 3(a). From the plot it is seen that the actual focal length is 26.9 mm, 1.1% shorter than the design length. The magnitude of the pressure is normalized to the value at the actual focal point. The depth of focus, defined as the distance between the points at which the pressure is 3 dB below that at the focal point, is about 4 mm. Of interest is the significant subsidiary focus formed within the near-field, which is a result of the phase sampling inherent to a Fresnel lens [8]. Defining the zones according to Eq. (1) for a phase plate yields a phase sampling rate of only twice per period.

The calculated on-axis profiles are shown in Figs. 3(b) and 3(c) for the lens operating at 8 and 12 MHz, respectively. It is seen that the focal length increases with increasing frequency as does the depth of focus. The change in the focal length with frequency is predicted by Eq. (1). The magnitude of the subsidiary focus becomes larger, relative to the main focus, with increasing frequency. To further investigate the behavior of the subsidiary focus, the on-axis prifile was plotted for a 4 zone, 11 mm diameter lens designed for the same center frequency and focal length as the 15 mm lens. Thus the F-number is increased to 2.36. The profile is shown in Fig. 4. From the plot it is apparent that the magnitude of the subsidiary focus becomes comparable to that of the main focus as the number of zones is decreased. In addition, the deviation of the true focal length from the design value increases as the number of zones is reduced. For the 11 mm zone plate, the actual focal length is 26.2 mm, 3.7% shorter than the design length.

The frequency independent focal plane profile for the 15 mm zone plate is shown in Fig. 5. The profile for an ideal spherical lens with the same focal length and diameter is shown also. It is seen that even for 7 zones the ideal profile is a reasonably good approximation. The 3 dB beamwidth for the zone plate is about 0.3 mm, and the magnitude of the first side-lobe is about 18 dB below that at the focal point.

IV. Construction and Performance Testing of A 15 mm Zone Plate

The 7 zone, 15 mm diameter zone plate described in the previous section was fabricated using 110 μm thick PVDF with gold electrodes. The FZP pattern was etched photolithographically. Since the features of the pattern are relatively large (on the order of 1 to 10 mils), an inexpensive laser-generated photoplot was used as a mask. Using a compresion jig, the PVDF was affixed to a polished composite backing material consisting of casting epoxy and tungsten dust of 2.15 μm average particle size. The volume percent of tung-

sten required to achieve an acoustic impedance match to the PVDF was calculated using the Reuss model for the bulk modulus of composite materials [9]. The transducer and backing material were housed in a plexiglas case, and electrical contacts from the electrodes to a coaxial cable were made using silver epoxy. Three more identical lenses were fabricated in the same manner.

The zone radii of the mask used to expose the FZP pattern were measured, and it was found that there were significant deviations from the desired values, especially in the outermost regions, due to the limited resolution of the laser-generated artwork. Beam profiles were calculated using the measured values. The focal length deviated from the ideal case by less than 2%, and the focal plane profile exhibited only minor differences.

In order to investigate the focusing ability of the lenses, two identical lenses were positioned in a water tank parallel to one another, separated by the appropriate confocal distance at 8, 10, and 12 MHz. At each frequency, a gated RF signal was transmitted by one of the lenses as it was scanned orthogonal to and through the lens axis. The voltage developed across the terminals of the receiving lens was recorded as a function of distance from the axis. Since the lenses are identical, the received voltage versus distance plot is proportional to the self-convolution of the focal plane profile of a single lens [10]. PVDF is very susceptible to electromagnetic interference, and a significant amount of RF feed-through was observed, making it difficult to isolate the delayed acoustic signal on an oscilloscope trace. The receiving lens was shielded with an aluminum cage fitted with a silver-painted mylar acoustic window, making it possible to isolate and trigger on the acoustic signal.

The Normalised received voltage plots are shown in Fig. 6. Since the focal plane profile is well-approximated by the ideal lens profile, it is expected that the self-convolution should resemble the pressure profile with little spreading. The experimental plots, however, are significantly wider than the calculated focal plane profile. In addition there is a lack of symmetry about the lens axis, especially at 8 MHz. Although some aberration effects are expected, it is not believed that it is the cause of the deviation in the experimental results. The measurement system offered no vernier control over the orientation of the lens faces. The lack of symmetry in the data suggests that the lenses were not parallel. The data, however, gives evidence of focusing, but it is impossible to make a meaningful quantitative assessment of the performance with the present measurement system. Currently, efforts are in progress to retrofit the measurement system with the necessary vernier control to generate accurate profiles.

V. Summary

In this paper theoretical beam profiles were generated for Fresnel zone plates. The on-axis profiles revealed the presence of significant subsidiary focci, which become increasingly larger in magnitude relative to the main focus as the number of zones is reduced. The focal plane response for a 7 zone lens was shown to be fairly well-approximated by the ideal profile.

The construction of a 7 zone, 15 mm PVDF zone plate was discussed, and experimental self-convolution results were presented. Limitations of the present measurement system are believed to be responsible for the poor results, and no quantitative assessment of the focusing performance was made. Efforts are in progress to improve the measurement system.

Acknowledgements

This work was supported by the American Heart Association and the National Institute of Health.

References

[1] L. F. Brown, "Electromechanical modeling, performance testing, and design of piezoelectric polymer film ultrasound transducers," Ph. D. dissertation, Iowa State Univ., Ames, IA, 1988.

[2] F. A. Jenkins and H. E. White, *Fundamentals of Optics*, 4th Ed., New York: McGraw-Hill, 1976.

[3] M. Mortezaie and G. Wade in *Acoustical Imaging*, M. Kaveh, R. K. Mueller, and J. F. Greenleaf, editors, vol. 13, New York: Plenum Press, 1984.

[4] K. Yamada and H. Shimizu, "New types of ultrasound focusing transducer systems," *Proc. of the Second Symposium on Ultrasonic Electronics*, Tokyo, 1981, *Japan J. Appl. Phys.*, vol. 21, suppl. 21-3, pp. 135-137, 1982.

[5] K. Yamada, H. Shimizu, and M. Minakata, "Planar-structure focusing lens for operation at 200 MHz and its application to the reflection-mode acoustic microscope," *IEEE Ultrasonics Symposium*, pp. 745-748, 1986.

[6] B. Noorbehesht, M. Mortezaie, G. Wade, and C. Schueler, in *Acoustical Imaging*, J. Powers, editor, vol. 11, New York: Plenum Press, 1981.

[7] B. Noorbehesht, G. Flesher, and G. Wade in *Ultrasonic Imaging*, vol. 2, Academic Press, Inc., 1980.

[8] G. S. Kino, *Acoustic Waves: Devices, Imaging, and Analog Signal Processing*, New Jersey: Prentice-Hall, Inc., 1987.

[9] M. G. Grewe, T. R. Gururaja, R. E. Newnham, and T. R. Shrout, "Acoustic properties of particle/polymer composites for transducer backing applications," *IEEE Ultrasonics Symposium*, pp. 713-716, 1989.

[10] W. Dürr, D. A. Sinclair, and E. A. Ash "A high resolution acoustic probe," *IEEE Ultrasonics Symposium*, pp. 594-597, 1980.

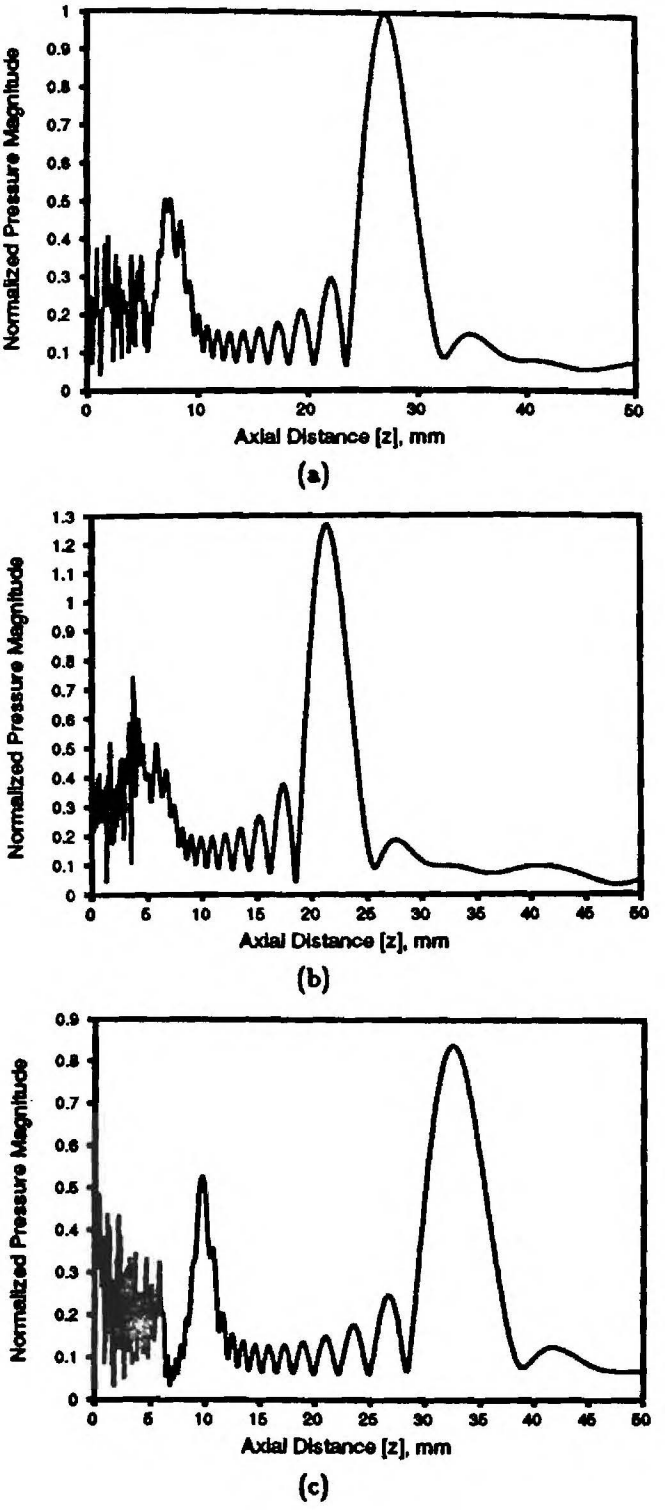

Figure 3: On-axis pressure profiles for a 7 zone, 15 mm diameter zone plate at 10 MHz (a), 8 MHz (b), and 12 MHz (c). Plots normalized to pressure at 10 MHz focal point.

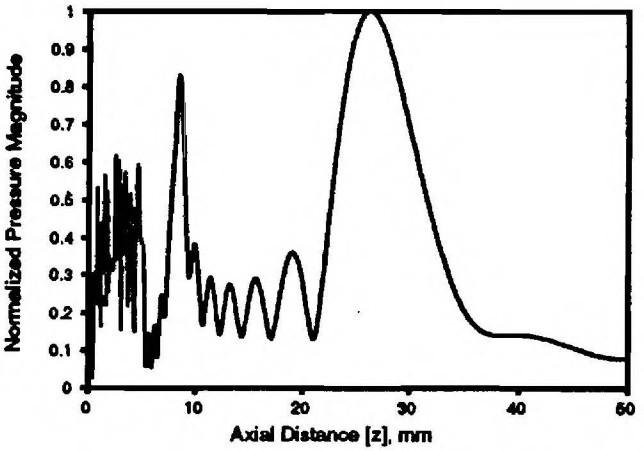

Figure 4: On-axis pressure profile for a 4 zone, 11 mm diameter zone plate.

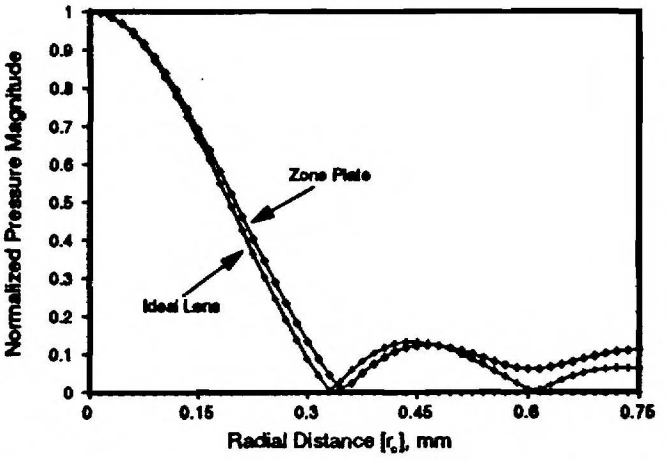

Figure 5: Focal plane pressure profiles for a 7 zone, 15 mm diameter zone plate and ideal lens.

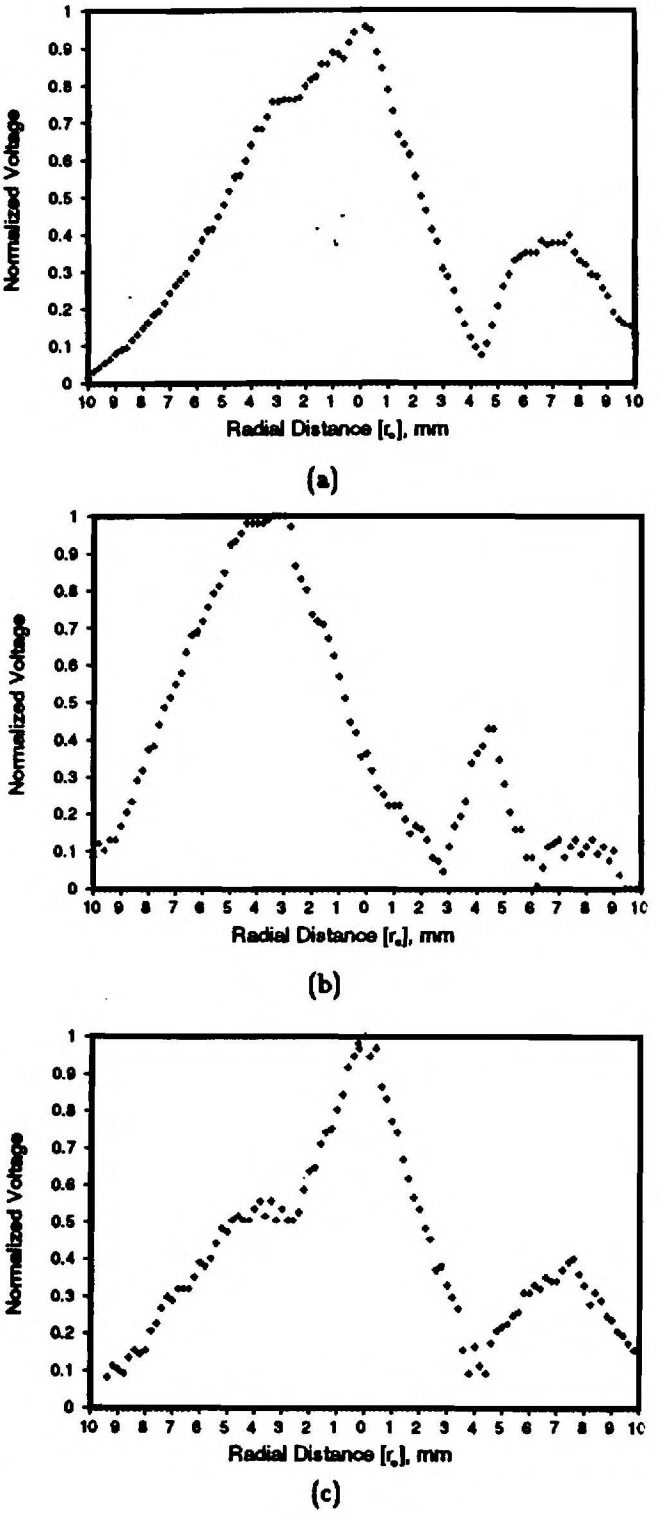

Figure 6: Normalised output voltage vs. distance off-axis at 10 MHz (a), 8 MHz (b), and 12 MHz (c).

TRANSIENT ANALYSIS OF A PVDF FRESNEL ZONE PLATE

M. Z. Sleva and W. D. Hunt

School of Electrical Engineering and Microelectronics Research Center
Georgia Institute of Technology, Atlanta, Georgia 30332-0250, USA

Abstract– **In this paper a method of estimating transient beam profiles for polyvinylidene fluoride (PVDF) Fresnel zone plates is presented. The plane and edge wave convolution integral approach is used to calculate the pressure, $p(t,\bar{r})$, at an arbitrary point due to the transient pressure, $p_o(t)$, at the front surface of the zone plate. This technique exploits the circular symmetry of the device to generate an analytic expression for the spatial impulse response, $h(t,\bar{r})$. Theoretical estimates of $p_o(t)$ are obtained using a lossy Mason model, which makes it possible to investigate the effects of various excitation signals on the beam profiles during the design phase. The dielectric and mechanical loss parameters used in the model are estimated from simple input impedance measurements of an air-backed, air-loaded sample of PVDF. Model results are presented for a 3-zone Fresnel zone plate, demonstrating the utility of the analysis in excitation signal design.**

1. Introduction

An acoustic Fresnel zone plate can be realized by depositing a zone plate electrode pattern on the front of a disk-shaped transducer while maintaining a full electrode on the back [1], as illustrated in fig. 1. The zone radii are determined from Fresnel diffraction theory [2] and are given by

$$r_m = \sqrt{\frac{m\lambda}{2}\left(z_o + \frac{m\lambda}{8}\right)} \;; \quad m = 1,3,5,\ldots \qquad (1)$$

where z_o is the focal length, and λ is the acoustic wavelength in the medium into which the device is radiating. The problem addressed in this work is that of developing a model for the zone plate transducer which can be used to predict the pressure waveform at a point in the field of the device when it is excited by an arbitrary signal. This work is motivated by an interest in investigating various wideband signals for potential use in a catheter-based tissue characterization system using a focused transducer. The approach taken by the authors is to treat independently the electromechanical model of the PVDF film and the acoustic model of the zone plate radiator.

The Mason model, modified to account for dielectric and mechanical losses, is used to develop a transfer function relating the pressure, $P_o(\omega)$, at the face of the transducer to the exciting voltage $V(\omega)$. The zone plate radiator is modeled as a series of concentric ring-shaped radiators and a center disk-shaped radiator mounted on an infinite rigid baffle. The plane and edge wave analysis for baffled planar pistons is used to generate a general expression for the spatial impulse response, $h(t,\bar{r})$, of the zone plate. Finally, the transient pressure, $p(t,\bar{r})$, is obtained from the convolution of $h(t,\bar{r})$ with $p_o(t)$, where $p_o(t)$ is the inverse Fourier transform of $P_o(\omega)$. Thus the transient analysis can be carried out for a zone plate design once the loss properties are determined for a sample of the PVDF film from which the transducer is to be constructed.

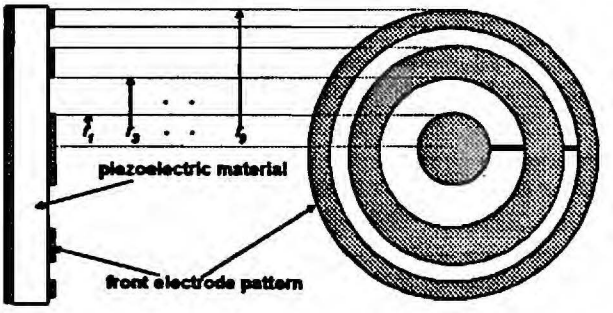

Fig. 1. Diagram of a 3-zone Fresnel zone plate transducer. Left, cross-sectional view; right, frontal view.

2. Electromechanical Model of the Transducer

The PVDF zone plate transducer is modeled as a lossy transducer of area A, equal to the total area of the zone plate electrode pattern. The Mason model, modified to account for dielectric and mechanical losses, is used.

Thus the zone plate transducer is assumed operating in thickness mode.

The relatively wide bandwidth of a properly designed PVDF transducer is due to the low acoustic impedance as well as the significant dielectric and mechanical losses associated with the material. The losses must be accounted for in the electromechanical model [3]. The classical Mason model (fig. 2) may be modified to account for dielectric and mechanical losses by making the substitutions [4],

$$\varepsilon^s \rightarrow \varepsilon^s(\omega)[1-j\varphi(\omega)] \qquad (2a)$$

$$c^D \rightarrow c^D(\omega)[1+j\psi(\omega)]\,, \qquad (2b)$$

where $\varepsilon^S(\omega)$ and $c^D(\omega)$ are the frequency dependent dielectric permittivity and elastic "constant", respectively. $\varphi(\omega)$ and $\psi(\omega)$ are the dielectric and mechanical loss tangents, respectively. Substitution (1a) results in replacing the bulk capacitance of the transducer, C_o, with the lossy capacitance, C_o^*, given by

$$C_o^* = \varepsilon^S(\omega)[1-j\varphi(\omega)]A/l \qquad (3)$$

for a transducer of area A and thickness l. The method of Brown and Carlson [5] is used to estimate $\varepsilon^S(\omega)$ and $\varphi(\omega)$ from input impedance measurements for an air-backed, air-loaded sample of PVDF over the frequency range of interest as follows:

Below resonance the input impedance of the sample is approximately that due to C_o^* so that

$$Z_{in} \approx \{\omega\varepsilon^S(\omega)[j+\varphi(\omega)]A/l\}^{-1}. \qquad (4)$$

Estimates of $\varepsilon^S(\omega)$ and $\varphi(\omega)$ can then be made using

$$\varphi(\omega) \approx -1/\tan(\theta_z) \qquad (5a)$$

$$\varepsilon^S(\omega) \approx l/\left\{|Z_{in}|\omega A\sqrt{\varphi^2(\omega)+1}\right\}, \qquad (5b)$$

where $|Z_{in}|$ and θ_z are the magnitude and phase of the input impedance, respectively. Since (5) do not hold near resonance, approximations for $\varepsilon^S(\omega)$ and $\varphi(\omega)$ must be obtained there by smoothly interpolating the results through resonance. Once $\varepsilon^S(\omega)$ and $\varphi(\omega)$ have been determined, the series resonant frequency, ω_s, can be estimated from the zero-crossing frequency of a least-squares linear fit to a plot of the reactive portion of the series impedance, Z_s, (fig. 2) versus frequency in the vicinity of resonance [5]. The acoustic velocity, v_l, is calculated using $v_l = \omega_s l/\pi$.

Substitution (1b) results in replacing the acoustic propagation constant, β_a, of the piezoelectric material with the complex acoustic propagation term, β_a^*, given by

$$\beta_a^* = \omega\sqrt{\rho_m/\{c^D[1+j\psi(\omega)]\}}$$

$$\approx \omega[1-j\psi(\omega)/2]\sqrt{\rho_m/c^D(\omega)}\,, \text{ for } \psi^2(\omega) \ll 1. \qquad (6)$$

In (6) ρ_m is the material density. If (6) is rewritten $\beta_a^* = \beta_a(\omega) - j\alpha(\omega) = \beta_a(\omega)[1-j\alpha(\omega)/\beta_a(\omega)]$, then $\psi(\omega)$ can be expressed in terms of the acoustic attenuation coefficient, $\alpha(\omega)$, as follows:

$$\psi(\omega) = 2\alpha(\omega)/\beta_a(\omega), \qquad (7)$$

where $\beta_a(\omega) = \omega\sqrt{\rho_m/c^D(\omega)}$.

The method of Turnbull *et al.* [6] is used to estimate α and the coupling coefficient, k_t, at ω_s from input impedance measurements. The assumption made in this work is that α and k_t are constant over the frequency range of interest and are equal to their respective values at ω_s. ψ is estimated at resonance using (7) with $\beta_a(\omega_s) = 4\pi/l$. ψ is assumed constant and equal to this value. Finally, the acoustic impedance, Z_o, is found using $Z_o = \rho_m\omega_s l/\pi$.

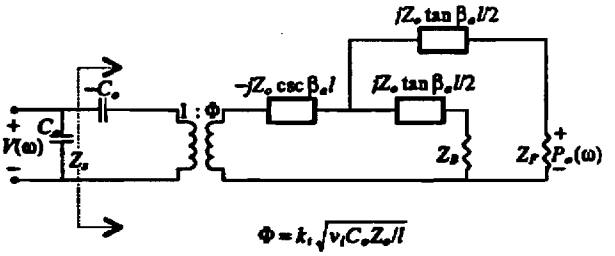

Fig. 2. The classical Mason model for a thickness-mode transducer terminated with acoustic impedances Z_F and Z_B.

3. Acoustic Model of the Zone Plate Radiator

The zone plate is modeled as a series of concentric annuli and a center disk vibrating as planar pistons mounted on an infinite rigid baffle. It has been shown [7] that PVDF transducers are well approximated by a simple piston model. The approach used to calculate the transient

field of the zone plate is the plane and edge wave convolution integral method of Lockwood and Willette [8], which is summarized here.

For an arbitrary point at $\bar{r} = r_c\hat{r}_c + z\hat{z}$ in the field of the device, the pressure, $p(t,\bar{r})$, due to the transient pressure, $p_o(t)$, at the surface of the radiator can be found using the convolution expression

$$p(t,\bar{r}) = \frac{1}{v_w}\frac{\partial}{\partial t}\Big(p_o(t) * h(t,\bar{r})\Big), \qquad (8)$$

where v_w is the speed of sound in the medium (taken to be water), and $h(t,\bar{r})$ is the spatial impulse response of the device. $h(t,\bar{r})$ can be found analytically for a disk radiator. For a point on the axis of symmetry (z axis) of a disk of radius a in the $z = 0$ plane, (8) reduces to

$$p(t,z) = p_o(t) * [\delta(\tau_1) - \delta(\tau_2)], \qquad (9)$$

where $\tau_1 = t - z/v_w$ and $\tau_2 = t - (z^2 + a^2)^{1/2}/v_w$. The interpretation of (9) is that the transient pressure is due to a plane wave originating at the center of the disk and an inverted "edge wave," each delayed by the appropriate travel time.

For the general case, it has been shown [7] that, for $r_c < a$, $h(t,\bar{r})$ is given by

$$\begin{aligned} h(t,\bar{r}) &= 0, \; v_w t < z \\ &= V_w, \; z < v_w t < R_1 \\ &= (v_w/\pi)\theta/2, \; R_1 < v_w t < R_2 \\ &= 0, \; v_w t > R_2, \end{aligned} \qquad (10a)$$

and, for $r_c \geq a$, by

$$\begin{aligned} h(t,\bar{r}) &= 0, \; v_w t < R_1 \\ &= (v_w/\pi)\theta/2, \; R_1 < v_w t < R_2 \\ &= 0, \; v_w t > R_2. \end{aligned} \qquad (10b)$$

In (10) $R_1 = \sqrt{(a - r_c)^2 + z^2}$, $R_2 = \sqrt{(a + r_c)^2 + z^2}$, and $\theta/2 = \cos^{-1}\{(r_c^2 + (v_w t)^2 - z^2 - a^2)/(2r_c\sqrt{(v_w t)^2 - z^2})\}$.

The analysis can be extended to treat an annulus with outer radius a and inner radius b by subtracting the impulse response of a disk of radius b from that of another disk of radius a [9]. Thus $p(t,\bar{r})$ due to a zone plate with N zones (N-1 annuli plus the center disk) can be expressed as

$$p(t,\bar{r}) = \frac{1}{v_w}\sum_{n=1}^{N}\left\{\frac{\partial}{\partial t}\Big(p_o(t) * h_n(t,\bar{r})\Big)\right\}, \qquad (11)$$

where $h_n(t,\bar{r})$ is the spatial impulse response of the n^{th} zone.

4. Results for a 3-Zone Fresnel Zone Plate

The transient analysis is demonstrated for a zone plate with three zones and a focal length of 5 mm. The diameter of the zone plate is 3.68 mm, resulting in an f-number of 1.36. The necessary material parameters used in the lossy Mason model were calculated from impedance measurements for an air-backed, air-loaded 1 cm^2 sample of PVDF using an HP 8753B network analyzer. The thickness of the sample was 109 μm, and the density was determined to be 1.86 g/cm^3. The relative permittivity and dielectric loss tangent curves are shown in fig. 4. Table 1 lists the remainder of the calculated material parameters for the sample. Assuming an impedance-matched backing ($Z_B = Z_o$) and water loading ($Z_F = 1.5$ MRayls), the transfer function $P_o(\omega)/V(\omega)$ was calculated for the zone plate transducer. The transient response was calculated for points along the z-axis for one-, three-, and six-cycle tone bursts of frequency $f_s = 2\pi\omega_s$ using (11), where $p_o(t)$ is the inverse Fourier transform of $P_o(\omega)$. The resulting transient beam profile for each case is shown in fig. 3.

For the case of one-cycle excitation, there is little near-field structure, and the focal region is poorly defined. For the three-cycle case, a well defined focus is present, and there is little near-field structure except for a subsidiary focus. Excitation with six cycles results in more near-field structure and a significant subsidiary focus. The focal plane profiles are shown in fig. 5. While the 3 dB beam width varies little with the number of cycles, the side lobe levels vary significantly, decreasing with increasing number of cycles. It can be concluded that for tone-burst excitation of a zone plate with N zones, the optimum number of cycles for a predictable on-axis profile is N. However, the number of zones should be large enough to sufficiently suppress the side lobes. It has been shown [1] that the focal plane profile of a 7-zone Fresnel zone plate approximates that of an ideal spherical lens with the same f-number reasonably well.

The authors are investigating a catheter-based tissue characterization system utilizing spread spectrum signal schemes. One excitation scheme of interest is the unweighted frequency modulated (FM) chirp given by

$$v(t) = \sin\left\{2\pi\left[f_{\min}t + \left(\frac{f_{\max}-f_{\min}}{T}\right)t^2/2\right]\right\}, \quad (12)$$

where $f_{max} - f_{min}$ is the frequency range of the chirp, and T is the duration of the signal. On-axis beam profiles for unweighted FM chirps from 8 to 12 MHz with T = 0.5 and 0.75 μsec and from 6 to 12 MHz with T = 0.75 μsec are shown in fig. 6. From fig. 6(a) it is evident that the chirp effectively extends the depth of focus for the zone plate. Further extension of the depth of focus can be achieved by increasing the duration of the chirp as in fig. 6(b). The magnitude of the near-field peak, however, is comparable to the focal region. Fig. 6(c) demonstrates that an increase in both the time duration and the frequency range, however, extends the depth of focus while limiting the magnitude of the near-field peak.

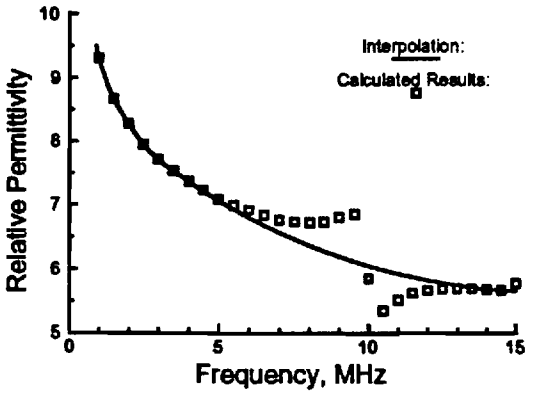

(a)

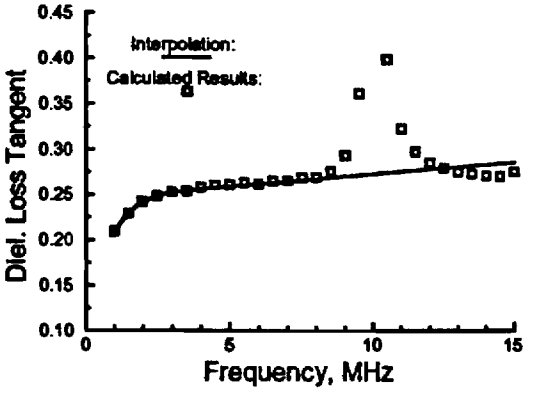

(b)

Fig. 3. Plots of (a) relative permittivity, $\varepsilon/\varepsilon_o$, and (b) dielectric loss tangent, φ, for the 109 μm thick PVDF.

In the preceding discussion it is demonstrated that the analysis presented in this work effectively enables the investigation of various excitation signal schemes; which, as illustrated in figs. 4, 5, and 6, can have a significant effect on the beam profile of a zone plate transducer. The excitation signal and zone plate, however, can be designed to optimize the shape of the profile for a particular application. Spread spectrum signals should be chosen to optimize both the signal processing and the acoustic performance of the system.

Z_o (MRayls)	v_t (km/s)	f_o (MHz)	Ψ	k_t
4.2	2.25	10.3	0.12	0.16

Table 1. Properties of the 109 μm thick PVDF.

5. Summary and Conclusion

A method of estimating transient beam profiles for PVDF Fresnel zone plates has been presented. This method uses the lossy Mason model for the transducer with the necessary material parameters determined from input impedance measurements on a sample of the material. The plane and edge wave analysis for baffled planar pistons is used for the zone plate acoustic radiator. This approach exploits the circular symmetry of the zone plate to obtain a general analytic expression for the spatial impulse response of the zone plate.

Theoretical beam profiles were calculated for a 3-zone device driven by tone-burst and unweighted FM chirp signals using material parameters for a sample of 109 μm thick PVDF. The results demonstrate the utility of the model in excitation signal design, which is of interest since the authors are investigating spread spectrum tissue characterization techniques. The results indicate that a signal scheme should be chosen with regard for both the signal processing and the acoustic requirements of the application.

Acknowledgements

This work was supported by the American Heart Association and the National Science Foundation.

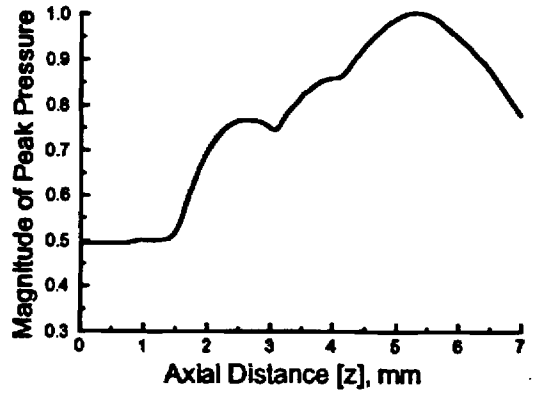

(a)

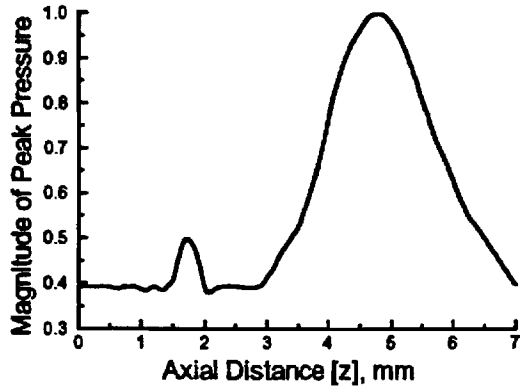

(b)

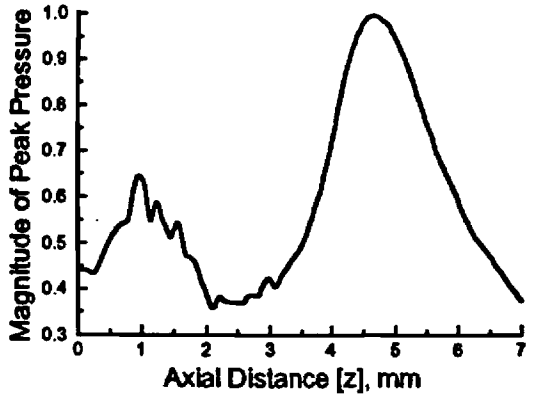

(c)

Fig. 4. Theoretical on-axis beam profiles for the 3-zone Fresnel zone plate excited by (a) one-cycle, (b) three-cycle, and (c) six-cycle tone bursts.

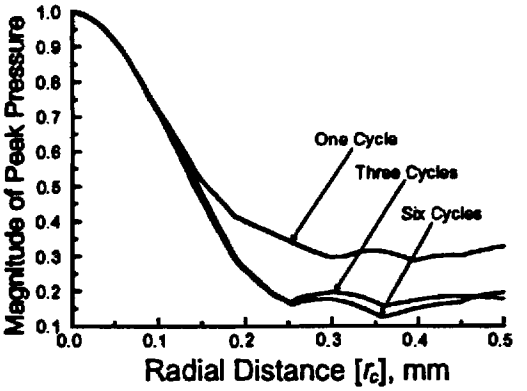

Fig. 5. Theoretical focal plane profiles for the 3-zone Fresnel zone plate excited by one-, three-, and six-cycle tone bursts.

References

[1] M. Z. Sleva and W. D. Hunt, "Design and construction of a PVDF Fresnel lens," *IEEE Ultrason. Symp.*, 1990, pp. 821-826.

[2] F. A. Jenkins and H. E. White, *Fundamentals of Optics*, 4th Ed., New York: McGraw-Hill, 1976.

[3] L. N. Bui, H. J. Shaw, and L. T. Zitelli, "Study of acoustic wave resonance in piezoelectric PVF_2 film," *IEEE Trans. Sonics Ultrason.*, vol. su-24, no.5, pp. 331-336, 1977.

[4] H. Ohigashi, T. Itoh, K. Kimura, T. Nakanishi, M. Suzuki, "Analysis of frequency response characteristics of polymer ultrasonic transducers," *Jpn. J. Appl. Phys.*, vol. 27, no. 3, pp. 354-360, 1988.

[5] L. F. Brown and D. L. Carlson, "Ultrasound transducer models for piezoelectric polymer films," *IEEE Trans. Sonics Ultrason.*, vol. 36, no. 3, pp. 313-318, 1989.

[6] D. H. Turnbull, M. D. Sherar, and F. S. Foster, "Determination of electromechanical coupling coefficients in transducer materials with high mechanical losses," *IEEE Ultrason. Symp.*, 1988, pp. 631-634.

[7] S. M. Kramer, S. L. McBride, H. D. Mair, and D. A. Hutchins, "Characteristics of wide-band planar ultrasonic transducers using plane and edge wave contributions," *IEEE Trans. Ultrason., Ferroelec. Freq. Contr.*, vol. 35, no. 2, 1988.

[8] J. C. Lockwood and J. G. Willette, "High-speed method for computing the exact solution for the pressure vibrations in the near field of a baffled piston," *J. Acoust. Soc. Amer.*, vol. 53, no. 3, pp. 735-741, 1973.

[9] D. A. Hutchins, H. D. Mair, and P. A. Puhach, "Transient pressure fields of PVDF transducers," *J. Acoust. Soc. Amer.*, vol. 82, no. 1, 1987.

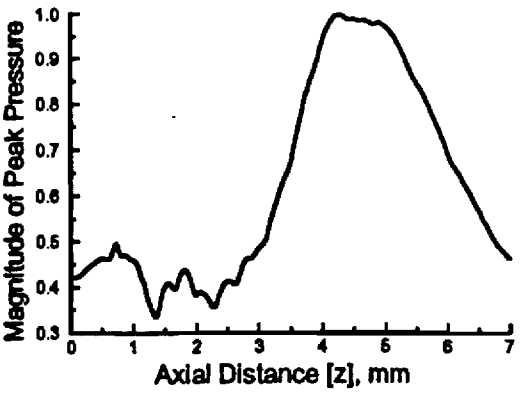

(a)

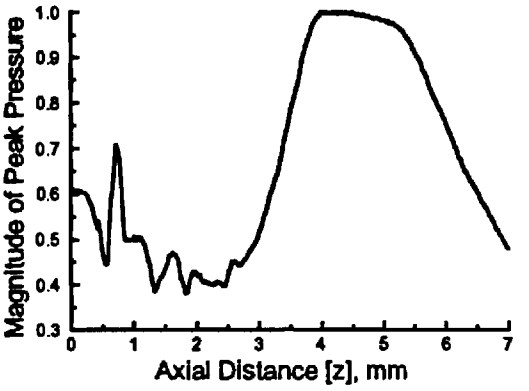

(b)

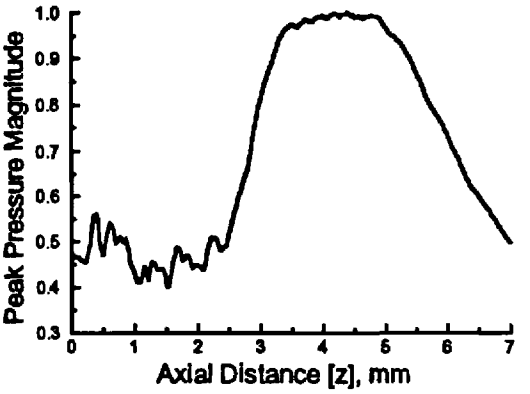

(c)

Fig. 6. Theoretical on-axis beam profiles for the 3-zone PVDF Fresnel zone plate excited by unweighted FM chirps. (a) 8 to 12 MHz, $T = 0.5$ μsec; (b) 8 to 12 MHz, $T = 0.75$ μsec; and (c) 6 to 12 MHz, $T = 0.75$ μsec.